

Ferroelectrically induced weak-ferromagnetism in a single-phase multiferroic by design

Craig J. Fennie

Center for Nanoscale Materials, Argonne National Laboratory, Argonne, IL 60439.

We present a strategy to design structures for which a polar lattice distortion induces weak ferromagnetism. We identify a large class of multiferroic oxides as potential realizations and use density-functional theory to screen several promising candidates. By elucidating the interplay between the polarization and the Dzyaloshinskii-Moriya vector, we show how the direction of the magnetization can be switched between 180° symmetry equivalent states with an applied electric field.

PACS numbers: 75.80.+q, 77.80.-e, 81.05.Zx

The rational design of new materials with emergent properties is a riveting challenge today in materials physics. It begins with understanding a mechanism to control the interplay between diverse microscopic degrees of freedom in order to create targeted macroscopic phenomena and ends with the discovery or design of new material realizations. When combined with first-principles density-functional theory, this approach provides an efficient strategy to survey the vast space of possible materials to target for synthesis. For example, new multiferroics in which magnetism coexists with ferroelectricity have been discovered where magnetic order itself induces ferroelectricity. Through this specific spin-lattice interaction, it is readily possible to control the direction of the electrical polarization with a magnetic-field [1, 2]. An equally fundamental but technologically more relevant problem that has received far less study is the electric-field control of magnetism [3, 4, 5, 6]. In particular, the electric-field switching of a magnetization between 180° symmetry equivalent states has yet to be demonstrated. The most promising direction to achieve this in single-phase materials involves a ferroelectric distortion inducing weak-ferromagnetism [7, 8, 9, 10]. Discovering a prototypical structure for which this approach might be realized, however, has remained elusive.

Weak-ferromagnetism (wFM) is the phenomenon whereby the predominantly collinear spins of an antiferromagnet cant in such a way as to produce a residual magnetization (\mathbf{M}). It can arise as a relativistic correction to Anderson's superexchange, i.e., the Dzyaloshinskii-Moriya (DM) interaction [11, 12], $E_{\text{DM}} = D_{ij} \cdot \mathbf{S}_i \times \mathbf{S}_j$ where D is the Dzyaloshinskii vector. A ferroelectric (FE) distortion can induce wFM when the phenomenological invariant $E_{\text{PLM}} \sim \mathbf{P} \cdot (\mathbf{L} \times \mathbf{M})$ is allowed in the energy of the antiferromagnetic-paraelectric (AFM-PE) phase, where \mathbf{P} and \mathbf{L} are the polarization and AFM vector respectively. Due to this term a coupling between the sign of \mathbf{P} and \mathbf{M} , for fixed \mathbf{L} , is evident. It is important to realize that a FE can still exhibit wFM without the FE distortion per se causing the wFM, i.e., without E_{PLM} in the corresponding PE phase. For example, although BiFeO_3 (the most widely studied multiferroic) can display wFM, such an invariant does not exist

as previously shown from explicit first-principles calculations [13] and as we argue below from symmetry. The challenge then is understanding how to start with the microscopic properties of E_{DM} and build a material capturing the macroscopic physics of E_{PLM} . In this Letter we present for the first time design criteria that facilitate this process. In general the criteria target a structure for which wFM is symmetry-forbidden in the PE phase but symmetry-allowed in the FE phase [4, 13]. Below we use this to identify a class of multiferroic oxides as potential realizations and use density-functional theory to screen several promising candidates. One complication arises in magnetic systems with broken spatial inversion such as a FE: a symmetry allowed interaction [14] may in some cases generate a long-wavelength magnetic spiral canceling the net \mathbf{M} , e.g., as in (bulk) BiFeO_3 . Here we consider the situation where this inhomogeneous state is suppressed, e.g., when single-ion anisotropy is large [15].

Our strategy is to formulate the problem in terms of a structural-chemical criterion and a magnetic criterion. To illustrate the idea we consider a two-sublattice antiferromagnet such as BiFeO_3 . A synopsis of the structural-chemical criterion is as follows: start with a PE structure, decorate the lattice with spins such that the midpoint between two spins coincides with a site having inversion (\mathcal{I}) symmetry (so that $D = 0$ by symmetry, i.e., Moriya's first rule [12]), place a FE-active ion at an \mathcal{I} -site. Compounds which satisfy this criterion are quite intriguing because if there are no other symmetry elements that would forbid wFM – the magnetic criterion – all that is required to induce a non-zero D and wFM is to remove the \mathcal{I} center by controlling the off-centering of the FE-active ion either by temperature, pressure, or electric-field. The magnetic criterion is primarily a question of how the spins order and of their direction with respect to the crystallographic axes. Notice our microscopic based criteria implies that \mathbf{L} is odd under \mathcal{I} , which is precisely what is required considering macroscopic phenomenology, i.e., E_{PLM} . These criteria facilitate evaluating known compounds or when combined with crystal chemistry principles designing new prototypes. For example, using PE BiFeO_3 as a starting point, we apply them to design a novel structure.

In PE BiFeO_3 , crystallographic space group $R\bar{3}c$, the

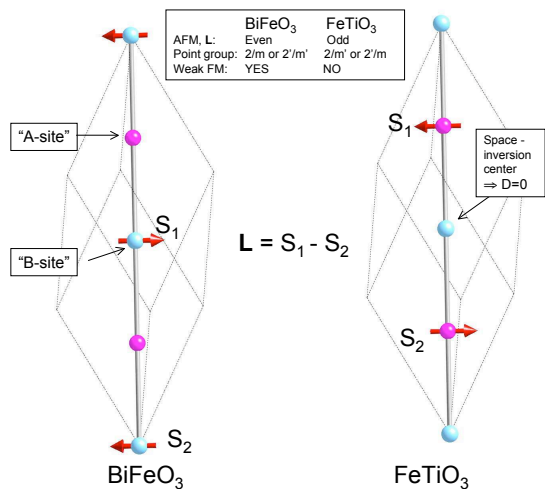


FIG. 1: Paraelectric ABO₃ compounds, space group, R $\bar{3}c$, BiFeO₃ and FeTiO₃. A-site: Wyckoff position 2a, site symmetry $\bar{3}2$. B-site: Wyckoff position 2b site symmetry, $\bar{3}$.

Bi-ions occupy the A-site, Wyckoff position 2a, with local site symmetry $\bar{3}2$, while the magnetic Fe-ion occupies a site with inversion symmetry, the B-site, position 2b, site symmetry $\bar{3}$. The Fe-spins order ferromagnetically within antiferromagnetically coupled (111) planes with the magnetic easy axis perpendicular to [111]. Although PE BiFeO₃ satisfies the magnetic criterion, $\mathcal{I}\mathbf{L}$ transforms each Fe sublattice onto itself, $\mathcal{I}\mathbf{L} = \mathcal{I}(S_1 - S_2) = \mathbf{L}$, as can be seen in Fig. 1(a). In this case of B-site magnetism the structural-chemical criterion is not met and the invariant E_{PLM} is forbidden by symmetry (the PE point group is $2'/m'$ or $2/m$ for which wFM is allowed). In contrast, consider the case where the magnetic ion is on the A-site and similarly ordered so that the magnetic criterion is still satisfied, Fig. 1(b). Now, in this case of A-site magnetism, $\mathcal{I}\mathbf{L} = -\mathbf{L}$. Placing a FE-active ion such as Ti⁴⁺ on the B-site would then satisfy the structural-chemical criterion. The PE magnetic point group is now $2/m'$ ($2'/m$) in which wFM is forbidden and *by design* a FE distortion, via E_{PLM} , would lower the symmetry to m' (m) thereby inducing wFM. The question remaining is whether compounds in our rationalized structure can be synthesized? As we discuss next, several already exist.

The mineral Ilmenite FeTiO₃ is one member of a family of compounds [16] that include the titanantes $A^{2+}Ti^{4+}O_3$ with $A = Mn-Ni$. They are all AFM insulators with ordering temperatures $T_N \sim 40K-100K$. At atmospheric pressure they form in the Ilmenite structure, space group R $\bar{3}$. Ilmenite can be thought of as an ordered corundum structure. At high-pressure both MnTiO₃ and FeTiO₃ have been found to form a quenchable metastable LiNbO₃ LBO-phase, space group R3c [17, 18]. Note this LBO-phase is structurally isomorphic to BiFeO₃ except the magnetic and FE atom positions are reversed, for example: MnTiO₃→BiFeO₃ implies Mn→Bi and Ti→Fe.

This is precisely the structural-chemical criterion outlined above. The remaining question is to identify the magnetic ground state in the FE phase to determine if the magnetic criterion is satisfied. In the remainder of this Letter we present a first-principles study of the FE and magnetic properties of the LBO-phase of MnTiO₃, FeTiO₃, and NiTiO₃. We demonstrate that these are realizations of the design criteria and provide a novel simple picture of how the interplay of D and \mathbf{P} leads to electric-field control of wFM.

Method.— We performed density-functional calculations using PAW potentials within LSDA+U [19] as implemented in VASP [20, 21]. The wavefunctions were expanded in plane waves up to a cutoff of 500 eV. Integrals over the Brillouin zone were approximated by sums on a $6 \times 6 \times 6$ Γ -centered k -point mesh. Phonons were calculated using the direct method. Where noted, non-collinear calculations with L-S coupling were performed. To find appropriate values of on-site Coulomb U and exchange J_H parameters we performed a series of calculations to estimate the Curie-Weiss temperature Θ_{CW} as a function of U for MnTiO₃, FeTiO₃, and NiTiO₃ in the *ground state Ilmenite structure*, space group R $\bar{3}$ [22]. For all compounds a value of $U = 4.5$ eV and $J_H = 0.9$ eV was found to give a reasonable account of the measured values. It should be noted that the presented results do not qualitatively change for reasonable variations of U .

Ferroelectricity.— In the soft-mode theory of ferroelectricity, the PE to FE transition is associated with the softening of a single unstable infrared-active phonon. In the R $\bar{3}c$ →R3c transition, this is a PE phonon polarized along [111] of symmetry type A_{2u} . We calculated the frequencies of these A_{2u} phonons at $T=0$ and found one highly unstable mode, e.g., in MnTiO₃, $\omega_{soft} \approx i150$ cm⁻¹. The character of this soft mode consists of A-ion and Ti displacements moving against oxygen, similar to

TABLE I: Theoretical (experimental) properties of multiferroic ATiO₃, space group R3c. *f.u.* \equiv formula unit.

	Mn (Exp. [17])	Fe (Exp. [18])	Ni
a_h	5.127Å (5.205Å)	5.05Å (5.12Å)	4.93Å
c_h	13.63Å (13.70Å)	13.52Å (13.76Å)	13.65Å
θ_r	56.4° (56.8°)	56.2° (56.0°)	54.7°
T_{FE}	>1000K	>1000K	>1000K
\mathbf{P}	83 $\mu C/cm^2$	94 $\mu C/cm^2$	110 $\mu C/cm^2$
Θ_{CW}	-290 K	-305 K	-170 K
T_N	135 K	260 K	100 K
\mathbf{L}	4.5 $\mu_B/f.u.$	3.6 $\mu_B/f.u.$	1.6 $\mu_B/f.u.$
\mathbf{M}	-0.002 $\mu_B/f.u.$	-0.03 $\mu_B/f.u.$	0.25 $\mu_B/f.u.$
J_1	-0.5meV	-1.0meV	-1.5meV
K	-0.02meV/ <i>f.u.</i>	-0.74 meV/ <i>f.u.</i>	-0.03 meV/ <i>f.u.</i>
D	-0.0004 meV/ <i>f.u.</i>	-0.02 meV/ <i>f.u.</i>	-0.35 meV/ <i>f.u.</i>

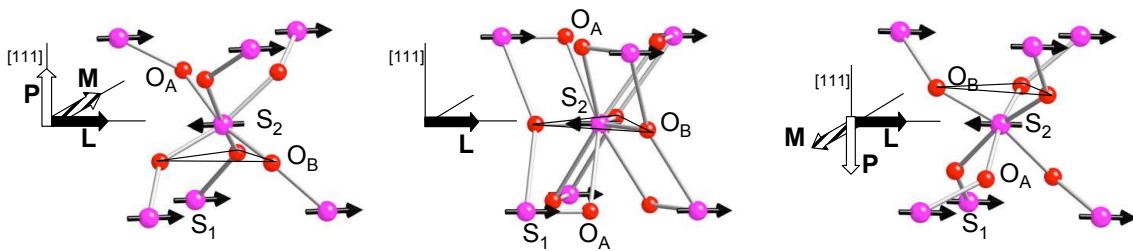


FIG. 2: Chiral nature of the S_1 -O- S_2 bonds; (Left) Polarization-up and (Right) Polarization-down. (Middle) Paraelectric state showing two equivalent *inter*-planar pathways, e.g. S_1 - O_A - S_2 and S_1 - O_B - S_2 . Note: $\mathbf{D} \parallel \mathbf{P}$, $\mathbf{L} \perp \mathbf{M} \perp \mathbf{P}$.

other R3c FEs such as BiFeO_3 and LiNbO_3 .

Next we broke inversion symmetry and performed a full structural optimization within the R3c space group. In Table I the calculated lattice constants at $T = 0$ are shown to be in excellent agreement with those observed at room temperature for MnTiO_3 and FeTiO_3 (R3c NiTiO_3 has not yet been synthesized.) The distortion leading from the PE to the FE structure can be decomposed entirely in terms of the soft-mode. The atomic displacements are almost equal in magnitude to those in LiNbO_3 , meeting Abraham's structural criteria for switchable ferroelectricity [23]. Based on Abraham's empirically derived formula relating the magnitude of these distortions to the FE transition temperature [23], we estimate FE $T_C \sim 1500\text{K}-2000\text{K}$. Finally, using the modern theory of polarization [24] we calculated a large $\mathbf{P} \approx 80-100 \mu\text{C}/\text{cm}^2$ comparable to that of BiFeO_3 .

Magnetic structure.— Weak ferromagnetism arises as a small perturbation - from the relativistic spin-orbit interaction - to a predominately collinear magnetic state, i.e., $|J| \gg |D|$, where J and D are Heisenberg and DM exchange respectively. This difference in energy scales naturally separates the problem. As such we first identify the collinear state that minimizes the spin-interaction energy without L-S coupling, i.e., $E_H = -\sum_{ij} J_{ij} \mathbf{S}_i \cdot \mathbf{S}_j$, by extracting the first four nearest neighbor (n.n.) exchange integrals, J_n , from total energy calculations [22]. We found the state that minimizes E_H consists of spins aligned ferromagnetically within antiferromagnetically coupled (111) planes, consistent with the magnetic criterion outlined above. This magnetic state arises due to a strong AFM J_1 coupling between n.n. spins in adjacent (111) planes. The Néel temperature calculated within mean-field theory [25] was found to be $T_N \sim 100\text{K}$ for MnTiO_3 and NiTiO_3 and $T_N \sim 250\text{K}$ for FeTiO_3 .

For a uniaxial crystal the orientation of the global spin axis relative to the crystallographic axis is given to lowest order by $E_{\text{ani}} = \sum_i K_i \sin^2(\theta)$, where θ is the angle between [111] and \mathbf{L} . Depending on the sign of K , the spins lie in a plane perpendicular or parallel to [111], in which case wFM is allowed or forbidden, respectively. To calculate the single-ion anisotropy constant K we first performed a self-consistent density-functional calculation

with collinear spins, without L-S coupling. Then, using the charge density and wavefunctions, we performed a series of non-selfconsistent calculations with spin-orbit interaction included for different orientations of the global spin axis. We found that the magnetic easy axis lies in the plane perpendicular to [111] with K ranging from -0.03 meV for MnTiO_3 and NiTiO_3 , to -0.7 meV for FeTiO_3 (the much large anisotropy for FeTiO_3 is associated with the orbital degeneracy). Symmetry then allows an additional contribution to the total energy which can cause the spins to cant: $E_{\text{DM}} = \sum_{ij} \tilde{D}_{ij} \cdot (\mathbf{S}_i \times \mathbf{S}_j)$, where \tilde{D}_{ij} is the Dzyaloshinskii vector. Phenomenologically this can be described by $E_{\text{DLM}} = \mathbf{D} \cdot (\mathbf{L} \times \mathbf{M})$ where $\mathbf{L} = \mathbf{S}_1 - \mathbf{S}_2$ and $\mathbf{M} = \mathbf{S}_1 + \mathbf{S}_2$. Symmetry requires \mathbf{D} to point along [111], i.e., parallel/antiparallel to \mathbf{P} . Since $K < 0$ requires \mathbf{L} to be in the plane perpendicular to [111] and subsequently to \mathbf{D} , the induced \mathbf{M} is perpendicular to \mathbf{P} . Once the direction of \mathbf{L} is fixed, the sign of \mathbf{M} that minimizes E_{DLM} is determined by the sign of \mathbf{D} .

Symmetry allows the spins to cant in the FE phase, but do they and by how much? To address this question we calculated the self consistent spin-density in the presence of the spin-orbit interaction for the FE structure with for example the polarization pointing down. The spins were initialized in a collinear configuration, e.g. $\mathbf{L}^0 = (2g\mu_B S, 0, 0)$, $\mathbf{M}^0 = (0, 0, 0)$, and then allowed to relax without any symmetry constraints imposed. For MnTiO_3 the induced moment was rather weak, $\mathbf{M} = (0, -0.002, 0) \mu_B/\text{formula unit (f.u.)}$, although comparable to the canonical weak-ferromagnet Fe_2O_3 and still measurable. The smallness of this result is not too surprising considering that the spin-orbit parameter λ vanishes for Mn^{2+} in the atomic limit. In contrast, λ is relatively large for Fe^{2+} and Ni^{2+} , and correspondingly the induced moments increase dramatically; $\mathbf{M} = (0, -0.03, 0) \mu_B/\text{f.u.}$ and $\mathbf{M} = (0, 0.25, 0) \mu_B/\text{f.u.}$ for FeTiO_3 and NiTiO_3 respectively [26]. Finally, we can approximate the strength of \tilde{D} from the calculated canting angle and J_1 . The results are summarized in Table I.

Next we proceed to elucidate the interaction between \mathbf{M} and \mathbf{P} . Similar calculations as we just discussed were performed for the PE structure and for the FE structure with \mathbf{P} in the opposite (symmetry equivalent) direction,

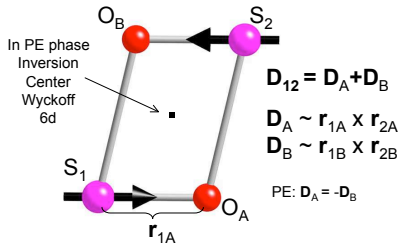


FIG. 3: Superexchange pathways, S_1 - O_A - S_2 and S_1 - O_B - S_2 , between nearest neighbor spins. The net Dzyaloshinskii-Moriya vector, \mathbf{D}_{12} , contains two contributions, \mathbf{D}_A and \mathbf{D}_B , that cancel in the paraelectric phase.

again relaxing the spin-density without symmetry constraints. In the former \mathbf{M} vanished confirming that the FE distortion is required for the observed wFM while in the latter \mathbf{M} switched sign. These results are consistent with our earlier symmetry arguments for a FE inducing wFM, i.e., for the invariant $E_{\text{PLM}} \sim \mathbf{P} \cdot (\mathbf{L} \times \mathbf{M})$ [27] and suggests that the direction of \mathbf{M} can be switched between stable 180° directions by an external electric field that would switch \mathbf{P} thereby switching \mathbf{M} . One way to understand this result is to argue that the sign of the DM vector \mathbf{D} depends on the direction of \mathbf{P} , i.e., $\mathbf{P} \propto \mathbf{D}$. At first this may seem puzzling considering the fact that D_{ij} is an axial vector. As Ederer and Spaldin pointed out [13], \mathbf{P} would have to change the sense of oxygen rotation in order for D to change sign. In Fig. 2 we compare the S - O - S bonds in the PE and up/down FE states, centering on spin S_2 and its nearest neighbors in adjacent (111) planes. A change in chirality of the S - O - S bonds is clearly visible due to a change in the direction of \mathbf{P} . The physics becomes clear by examining the microscopic E_{DM} and realizing that the net Dzyaloshinskii vector $\tilde{D}_{ij} = \sum_{\alpha} D_{ij}^{\alpha}$ has to be summed over all distinct S_1 - O_{α} - S_2 pathways. In the PE structure two pathways, a left and right chiral, contribute to \tilde{D}_{12} as we show in Fig. 3. The orientation of the D_{12}^A vector is given by [28, 29] $D_{12}^A \sim r_{1A} \times r_{2A}$ where r_{1A} is the unit vector pointing along the S_1 - O_A direction. There is, however, an additional pathway connecting S_1 to S_2 through O_B . In the PE phase D^A and D^B can be shown to have equal magnitude but opposite sign leading to a vanishing net DM interaction. In the FE phase, \mathbf{P} strengthens/weakens one pathway over the other leading to a finite DM interaction (in Fig. 2 we only show the “strong” S_1 - O - S_2 pathway in the FE phase). Therefore the origin of ferroelectrically-induced wFM in this class of materials is a change in the relative contribution of two DM superexchange pathways (with opposite sign) due to a polar lattice distortion.

Today, the challenge in multiferroics has shifted from finding new magnetic ferroelectrics to identifying materials in which the polarization and the magnetization are strongly coupled. In this work we have presented criteria that have the potential to advance the discovery of such

complex materials. These electrically-controlled switchable magnets provide fertile ground for additional studies of how spin and lattice degrees of freedom interact and also hold promise for application in magnetic devices.

Useful discussions with Matthias Bode, Venkat Gopalan, Darrell Schlom, and S.K. Streiffer are acknowledged. Work at the Center for Nanoscale Materials was supported by US DOE, Office of Science, Basic Energy Sciences under Contract No. DE-AC02-06CH11357.

-
- [1] S. -W Cheong and M. Mostovoy, *Nature Materials* **6**, 13 (2007).
 - [2] T. Kimura, *Annu. Rev. Mater. Res* **37**, 387 (2007).
 - [3] T. Lottermoser et al., *Nature* **430**, 541 (2004).
 - [4] C. Ederer and N. A. Spaldin, *Phys. Rev. B* **74**, 020401(R) (2006).
 - [5] T. Zhao et al., *Nature Materials* **5**, 823 (2006).
 - [6] Y. Yamasaki et al., *Phys. Rev. Lett.* **98**, 147204 (2007).
 - [7] D. L. Fox and J. F. Scott, *J. Phys. C: Solid State Phys.* **10**, L329 (1977).
 - [8] R. Ramesh and N. A. Spaldin, *Nature Materials* **6**, 21 (2007).
 - [9] W. Eerenstein, N. D. Mathur, and J. F. Scott, *Nature* **442**, 759 (2006).
 - [10] J. F. Scott, *Science* **315**, 954 (2007).
 - [11] I. Dzyaloshinskii, *J. Phys. Chem. Solids* **4**, 241 (1958).
 - [12] T. Moriya, *Phys. Rev.* **120**, 91 (1960).
 - [13] C. Ederer and N. A. Spaldin, *Phys. Rev. B* **71**, 060401(R) (2005).
 - [14] I. Dzyaloshinskii, *Soviet Physics JETP* **19**, 960 (1964).
 - [15] More generally, a spiral may be “unwound” [9] by doping, high magnetic fields, or strain. See for example: F. Bai et al., *Appl. Phys. Lett.* **86**, 032511 (2005).
 - [16] J. B. Goodenough and J. J. Stickler, *Phys. Rev.* **164**, 768 (1967).
 - [17] J. Ko and C. T. Prewitt, *Phys. Chem. Minerals* **15**, 355 (1988).
 - [18] L. C. Ming et al., *American Mineralogist* **91**, 120 (2006).
 - [19] V. I. Anisimov et al., *J. Phys.: Condens. Matt.* **9**, 767 (1997).
 - [20] G. Kresse and J. Hafner, *Phys. Rev. B* **47**, R558 (1993); G. Kresse and J. Furthmüller, *ibid.* **54**, 11169 (1996).
 - [21] P. E. Blöchl, *Phys. Rev. B* **50**, 17953 (1994); G. Kresse and D. Joubert, *ibid.* **59**, 1758 (1999).
 - [22] Total energy calculations for 10 linearly independent spin configurations were performed in an 80-atom supercell.
 - [23] S. C. Abrahams et al., *Phys. Rev* **172**, 551 (1968).
 - [24] R. D. King-Smith, and D. Vanderbilt, *Phys. Rev. B* **47**, R1651 (1993).
 - [25] J. Samuel Smart, *Effective Field Theories of Magnetism* (Saunders Company, Philadelphia 1966).
 - [26] The trend is also consistent with $\mathbf{D} \sim \Delta g \mathbf{J}$, where Δg is the change in the g-factor. See Refs. 12, 16.
 - [27] We performed further calculations with \mathbf{L} and \mathbf{P} initialized in several directions, all results are consistent with the symmetry of this interaction, i.e., $P_z(L_x M_y - L_y M_x)$.
 - [28] F. Keffer, *Phys. Rev.* **126**, 896 (1962).
 - [29] A. S. Moskvin, *JEPT* **104**, 913 (2007).